Generation of 131 fs mode-locked pulses from 2.8 μm Er:ZBLAN fiber laser

Hongan Gu (顾宏安), Zhipeng Qin (覃治鹏), Guoqiang Xie (谢国强)*, Ting Hai (海 婷), Peng Yuan (袁 鹏), Jingui Ma (马金贵), and Liejia Qian (钱列加)

School of Physics and Astronomy, Key Laboratory for Laser Plasmas (Ministry of Education), Collaborative Innovation Center of IFSA (CICIFSA), Shanghai Jiao Tong University, Shanghai 200240, China

**Corresponding author: xiegq@sjtu.edu.cn*

Received October 23, 2019; accepted December 11, 2019; posted online March 9, 2020

We demonstrated a femtosecond mode-locked Er:ZrF_4-BaF_2-LaF_3-AlF_3-NaF (Er:ZBLAN) fiber laser at 2.8 μm based on the nonlinear polarization rotation technique. The laser generated an average output power of 317 mW with a repetition rate of 107 MHz and pulse duration as short as 131 fs. To the best of our knowledge, this is the shortest pulse generated directly from a mid-infrared mode-locked Er:ZBLAN fiber laser to date. Numerical simulation and experimental results confirm that reducing the gain fiber length is an effective way to shorten the mode-locked pulse duration in the Er:ZBLAN fiber laser. The work takes an important step towards sub-100-fs mid-infrared pulse generation from mode-locked Er:ZBLAN fiber lasers.

Keywords: generation; mode-locked pulses; Er:ZBLAN fiber.
doi: 10.3788/COL202018.031402.

Mid-infrared (mid-IR) ultrafast laser sources are of particular interest for applications such as molecular spectroscopy, material processing, remote sensing, LIDAR, laser electron interaction, and high harmonics generation[1–9]. In the past, mid-IR ultrafast laser sources were mainly produced by nonlinear frequency conversion approaches such as an optical parametric oscillator (OPO) and an optical parametric amplifier (OPA)[10–12]. However, these nonlinear approaches are generally expensive and complex and require precise optical synchronization, which prevents their widespread application. In recent years, the mode-locked fluoride fiber laser (MLFFL) has emerged as a simple and economic way to directly generate ultrashort pulses in the mid-IR range[13–19]. Compared with OPO and OPA, diode-pumped MLFFL is more appealing to practical applications because of its compact structure, high efficiency, and excellent beam quality.

Among rare-earth-doped (Er^{3+}, Ho^{3+}, and Dy^{3+}) fluoride fiber lasers, an Er^{3+}-doped ZrF_4–BaF_2–LaF_3–AlF_3–NaF (ZBLAN) fiber laser around 2.8 μm attracts more attention due to its large stimulated emission cross section[20], compatibility with 970 nm diode pumping, and high laser efficiency[21]. Picosecond mode-locked Er:ZBLAN fiber lasers have been achieved using real saturable absorbers such as semiconductor saturable absorber mirrors (SESAMs), two-dimensional materials, and nonlinear mirrors[22–27]. Until 2015, the femtosecond mode-locked Er:ZBLAN fiber laser was reported using the nonlinear polarization rotation (NPR) technique, in which a 207 fs soliton pulse was produced[28]. The ultrashort pulse generation can be attributed to the combination of an ultrafast response of NPR action and the soliton shaping effect. Although several passively MLFFLs were demonstrated later using NPR[29–31], the pulse durations were remarkably beyond 200 fs. A shorter mode-locked pulse of 180 fs was obtained with a Ho–Pr co-doped ZBLAN fiber at 2.9 μm due to a broader gain linewidth and lower loss in atmosphere[13]. For some applications, such as supercontinuum generation, soliton self-frequency shift, pump-probe experiment, and chirped pulse amplification, an ultrashort mid-IR pulse with shorter duration is desired[32–36].

In this Letter, we demonstrated 131 fs mid-IR pulse generation from an NPR mode-locked Er:ZBLAN fiber laser by optimizing the gain fiber length. Comparison experiments show that reducing the gain fiber length helps to achieve shorter mode-locked pulses. By using a 1.61 m Er:ZBLAN fiber as the gain medium, we achieved stable mode-locked pulses with an average output power of 317 mW and a pulse duration of 131 fs at 2.8 μm. To the best of our knowledge, this is the shortest mode-locked pulse generated directly from a mid-IR Er:ZBLAN fiber laser. Numerical simulation also confirms that reducing the gain fiber length is an effective way to shorten pulse duration of MLFFL.

The passively mode-locked Er:ZBLAN fiber laser (Fig. 1) was pumped by a 970 nm laser diode (LD), which outputs through a pigtail fiber with a numerical aperture (NA) of 0.15 and core diameter of 105 μm. A set of lenses consisting of plano-convex lens L_1 and aspheric lens L_2 was used to couple the pump beam into the gain fiber. The gain fiber was a double-cladding 6 mol.% Er:ZBLAN fiber (FiberLabs) with a 20 μm core diameter (NA = 0.12) and a 200 μm cladding diameter. The absorption coefficient of the Er:ZBLAN fiber was measured to be 5.96 dB/m using the cut-back method. Both ends of the fiber were angle-cleaved to suppress the parasitic oscillation. Mode locking was achieved using the NPR technique. This artificial saturable absorber consisted of a half-wave plate, a quarter-wave plate (Altechna), and a polarization-dependent isolator (Thorlabs). To reduce

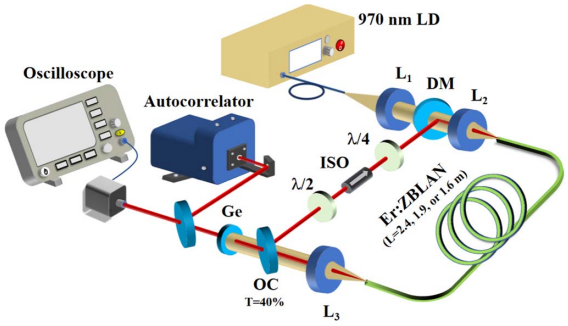

Fig. 1. Experimental setup of an NPR mode-locked Er:ZBLAN fiber laser. LD, laser diode; L_1, plano-convex lens ($f = 10$ mm); L_2 and L_3, aspheric ZnSe lenses ($f = 12.7$ mm); DM, dichroic mirror; Ge, germanium plate; OC, output coupler ($T = 40\%$); $\lambda/2$, half-wave plate; $\lambda/4$, quarter-wave plate; ISO, polarization-dependent optical isolator.

the mode-locking threshold, an intracavity pulse propagated along the pump light direction. The pulses were extracted from a 40% output coupler (OC) after the gain fiber. We filtered the residual pump light using a germanium plate. Output pulses were captured by a mid-IR photodetector (VIGO System, PCI-2TE-12) with a response time of ~7 ns around 2.8 μm and displayed on a 1 GHz digital oscilloscope (Tektronix, MDO3102). The output pulse spectrum was measured by a mid-IR optical spectrum analyzer (Ocean Optics, SIR5000) with a resolution of 0.22 nm. Pulse duration was measured by a commercial intensity autocorrelator (APE, PulseCheck150).

In the experiment, we performed the mode-locking experiments with three different gain fiber lengths ($L = 2.47$, 1.92, and 1.61 m). Experimental results are summarized in Table 1. In these cases, mode-locking operations could be self-started, but it had a higher mode-locking threshold for shorter fibers due to a higher pulse repetition rate and less nonlinear phase accumulation. It is worth noting that the propagation direction of the intracavity pulse will influence the mode-locking threshold. The intracavity pulse along the pump direction will grow rapidly and more easily accumulate the required nonlinear phase shift for initiating mode-locking operation. Compared with a previously reported mode-locking threshold of 17 W ($L = 1.6$ m and OC of 37%)[31], where the intracavity pulse propagated in the opposite direction of pump light, here, the mode-locking threshold was only 6.79 W with a 1.61 m gain fiber. The maximum average output power was obtained by increasing the pump power until pulse splitting occurred. Although the maximum average output power was higher (317 mW) with a 1.61 m fiber, the pulse energies were comparable (~3 nJ) for three fiber lengths, owing to different repetition rates. For three fiber lengths, stable continuous-wave mode locking was obtained, and the fluctuation of average output power was ~1%. Figure 2(a) shows the pulse trains of the mode-locked laser using a 1.61 m Er:ZBLAN fiber. Despite a slow response of the mid-IR photodetector, stable mode-locked pulse trains in nanosecond and millisecond time scales were observed. Using an RF spectrum analyzer, we observed the fundamental beat signal with a signal-to-noise ratio (SNR) of 71 dB at 106.7 MHz [Fig. 2(b)], indicating very stable mode locking. The inset of Fig. 2(b) shows the harmonic beats with a reduced intensity profile due to the finite photodetector bandwidth.

We investigated the mode-locked pulse duration variation with gain fiber length. Since soliton pulse duration is inversely proportional to pulse energy according to the soliton area theorem, in each case we recorded the mode-locked pulse duration at the highest pulse energy. In the meantime, we carefully optimized the waveplates for obtaining the shortest pulses in each case, and intensity autocorrelation traces fitted by sech^2-shaped profiles are shown in Figs. 3(a)–3(c) with three different gain fiber lengths.

The main pulses are fitted perfectly, while some secondary peaks are located at two wings, which originate from a resonant dispersive wave[37]. From Figs. 3(a)–3(c), it can be clearly seen that mode-locked pulse duration decreases significantly with shortening of the gain fiber. Using a 1.61 m gain fiber, the shortest pulse of 131 fs was achieved from the NPR mode-locked Er:ZBLAN fiber laser. The mode-locking spectra are presented in Figs. 3(d)–3(f), featuring typical Kelly sidebands. The spectral profiles show asymmetric sidebands, which are different from the typical shape of conventional solitons[38,39]. The asymmetric sidebands could be mainly attributed to the absorption of water vapor around 2.8 μm[28]. The mode-locking spectrum is remarkably wider in the case of the 1.61 m gain fiber. In the experiment, we could not achieve mode-locking while the gain fiber length was below 1.61 m due to insufficient gain. By increasing the Er-doping concentration in the fiber, it should be possible to mode lock with shorter gain fiber.

Since a fluoride fiber has an anomalous dispersion in the mid-IR band, femtosecond mode-locked Er:ZBLAN fiber lasers usually work in the soliton regime. The peak power

Table 1. Mode-Locking Experimental Results with Three Different Gain Fiber Lengths ($L = 2.47$, 1.92, and 1.61 m)

Length (m)	Threshold (W)	Pump Power (W)	Average Power (mW)	Rep. Rate (MHz)	Pulse Energy (nJ)	Duration (fs)	Peak Power (kW)
2.47	5.28	6.42	245	69.97	3.06	202	15.15
1.92	5.45	7.45	289	91.93	3.15	180	17.50
1.61	6.79	9.36	317	106.67	2.97	131	22.68

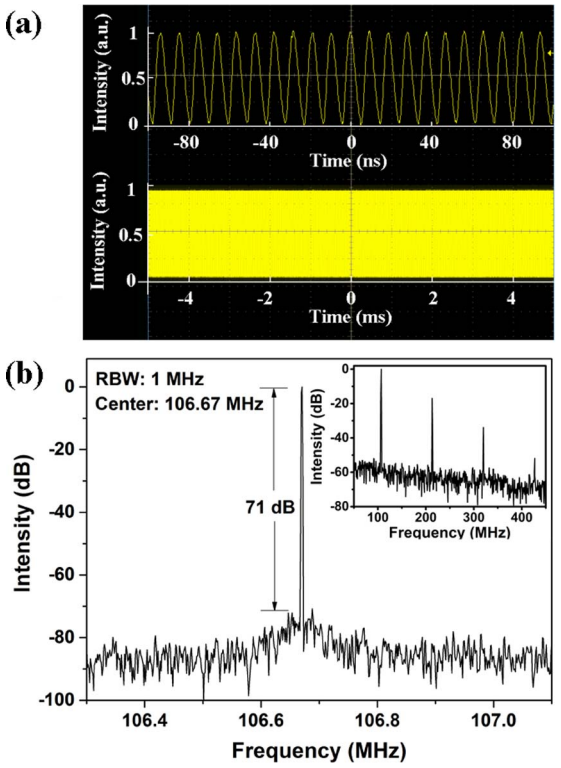

Fig. 2. (a) Measured mode-locked pulse trains using a 1.61 m Er:ZBLAN fiber. (b) Fundamental beat RF spectrum. Inset: harmonic beats RF spectrum. RBW, resolution bandwidth.

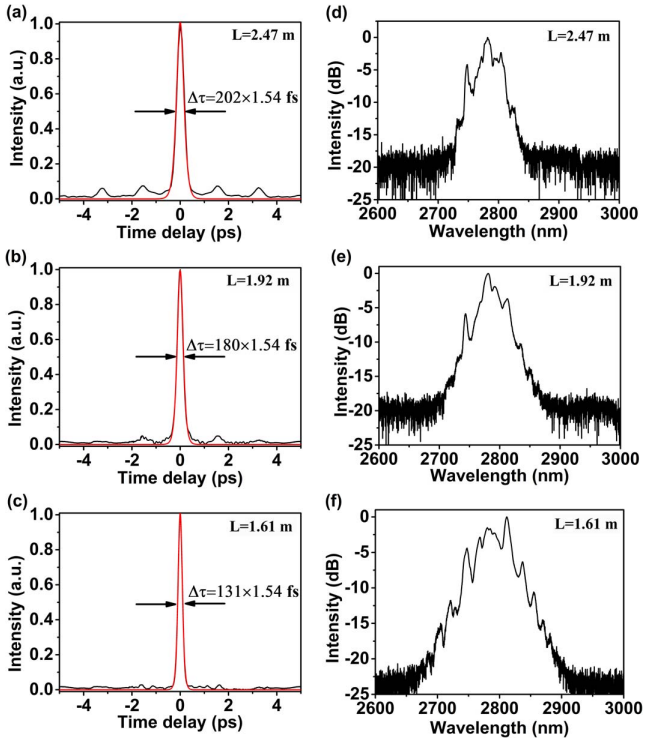

Fig. 3. (a)–(c) Pulse durations and (d)–(f) spectra obtained from mode-locked Er:ZBLAN fiber lasers with different gain fiber lengths of 2.47 m, 1.92 m, and 1.61 m, respectively.

of the soliton is clamped by the nonlinear phase shift accumulation in the cavity. Because the accumulated nonlinear phase shift is proportional to the product of the fiber length and peak power, a shorter gain fiber mode-locked laser is used to produce a higher peak power. As expected, the pulse peak power increased significantly from 15.15 kW to 22.68 kW by reducing the gain fiber length (Table 1). We measured the beam quality of the output laser with the knife-edge method. The M^2 factor is 1.5, as shown in Fig. 4.

The pulse shortening with the decrease of fiber length is attributed to the dispersion condition. The intracavity net anomalous dispersion will be reduced with a shorter fiber length, which helps to obtain shorter mode-locked pulses, as shown in solid-state and fiber soliton mode-locked lasers[40,41]. In fact, 724, 883, and ~1000 fs pulses were generated from the Dy:ZBLAN fibers with lengths of 3, 4.5, and 5.5 m, respectively[41].

In order to confirm the dependence of pulse width on gain fiber length in the mode-locked Er:ZBLAN fiber laser, we numerically simulated the evolution of pulse duration with gain fiber length by solving the modified nonlinear Schrödinger equation[42,43]:

$$\frac{\partial E}{\partial z}+i\frac{\beta_2}{2}\frac{\partial^2 E}{\partial \tau^2}-\frac{\beta_3}{2}\frac{\partial^3 E}{\partial \tau^3}=\frac{g}{2}E+i\gamma|E|^2E, \tag{1}$$

where E is the slowly varying amplitude of the pulse, z is the propagation coordinate, and τ is the time-delay

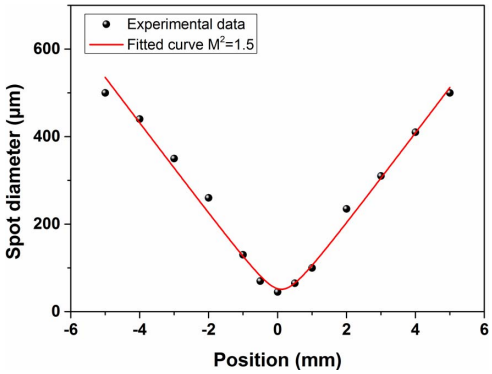

Fig. 4. Measurement results of beam quality.

parameter. $\beta_2=-83\,\mathrm{fs^2/mm}$ and $\beta_3=467\,\mathrm{fs^3/mm}$ are the group velocity dispersion and third-order dispersion of the Er:ZBLAN fiber, respectively[44]. $\gamma=1.45\times10^{-4}\,\mathrm{W^{-1}\cdot m^{-1}}$ is the nonlinearity parameter of the Er:ZBLAN fiber[45]. The gain is given by

$$g(\omega)=\frac{g_0}{1+\frac{E_p}{E_{\mathrm{sat}}}}\cdot\frac{1}{1+4\left(\frac{\omega-\omega_0}{\Delta\omega}\right)^2}, \tag{2}$$

where $g_0=8^{-1}$ m is the small signal gain coefficient[23], $E_p=\int|E|^2\mathrm{d}\tau$ is the intracavity pulse energy, ω_0 is the central angular frequency, and $\Delta\omega=29.2$ THz is the gain bandwidth. The saturation energy $E_{\mathrm{sat}}=E_{\mathrm{sat\_0}}\cdot\exp(-\alpha_p\cdot z)$ is proportional to the launched pump power

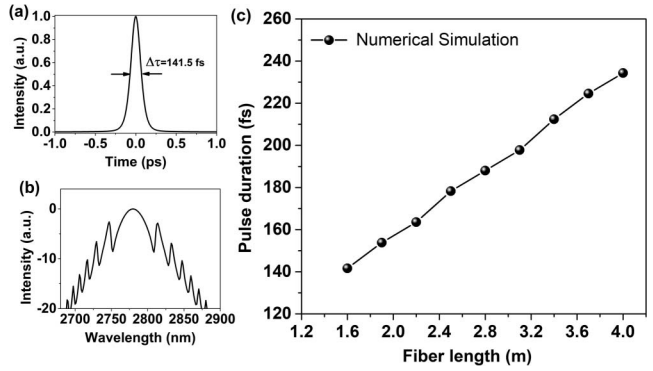

Fig. 5. (a) Calculated pulse profile and (b) spectrum with a fiber length of 1.6 m. (c) Pulse duration variation with the length of Er:ZBLAN gain fiber.

and decreases along the propagation distance. $\alpha_p = -1.373\ \mathrm{m}^{-1}$ is the absorption coefficient of fiber at the pump wavelength. The saturable absorber is modeled by a transmission function:

$$T = 1 - q_0 \Big/ \left(1 + \frac{|E|^2}{P_0}\right), \tag{3}$$

where the saturable loss q_0 and the saturation power P_0 are fixed to be 0.8 and 1 kW, respectively.

For each gain fiber length, we optimized the value of $E_{\mathrm{sat\_0}}$ for achieving the shortest pulse duration. Numerical simulation shows that stable solitons can be obtained with typical Kelly sidebands, as shown in Figs. 5(a) and 5(b). Limited by the soliton area theorem, intracavity pulse energy is finite. Soliton splitting and multi-pulse operation are observed when $E_{\mathrm{sat\_0}}$ is beyond a certain value. Before soliton splitting, we recorded the shortest pulse duration for each gain fiber length, as shown in Fig. 5(c). It can be clearly seen that the mode-locked pulse duration decreases with the reducing Er:ZBLAN fiber length, which coincides with the experimental results. The decrease of pulse duration with gain fiber length may be attributed to less net intracavity dispersion for shorter fibers. Anyway, reducing the gain fiber length is an effective way to shorten the pulse duration in mode-locked Er:ZBLAN fiber lasers. Sub-100-fs pulse generation is also expected from mode-locked Er:ZBLAN fiber lasers by adopting high-doping fibers and further reducing gain fiber length. Besides, dispersion management is also a promising way to achieve sub-100-fs mode-locked pulses[46].

Up to now, many low-dimension materials have been successfully demonstrated as effective saturable absorbers in the fiber lasers[43,47–51]. In fact, we also tried mode-locking of Er:ZBLAN fiber laser with black phosphorus, however, we can only obtain picosecond mode-locked pulses[25]. In the future, we will investigate other low-dimension materials as mode-lockers in the mid-IR spectral band where a saturable absorber is scarce.

In conclusion, we demonstrated a mode-locked Er:ZBLAN fiber laser at 2.8 μm. By optimizing the gain fiber length, the mode-locked pulse as short as 131 fs was directly generated from the Er:ZBLAN fiber laser with an average output power of 317 mW and a repetition rate of 107 MHz, corresponding to a pulse energy of 3 nJ and a peak power of 23 kW. To the best of our knowledge, this is the shortest mode-locked pulse reported on mid-IR MLFFLs. Our research results demonstrate that reducing the gain fiber length is an effective way to shorten pulse duration in MLFFLs. Such femtosecond mode-locked pulse sources are very appealing for applications of mid-IR supercontinuum generation, soliton self-frequency shift, and pump-probe experiments.

This work was supported by the National Natural Science Foundation of China (Nos. 61675130, 91850203, and 11721091) and the National Postdoctoral Program for Innovative Talents (No. BX20170149).

References

1. J. Ma, Z. Qin, G. Xie, L. Qian, and D. Tang, Appl. Phys. Rev. **6**, 021317 (2019).
2. E. Sorokin, I. T. Sorokina, J. Mandon, G. Guelachvili, and N. Picqué, Opt. Express **15**, 16540 (2007).
3. A. H. Nejadmalayeri, P. R. Herman, J. Burghoff, M. Will, S. Nolte, and A. Tünnermann, Opt. Lett. **30**, 964 (2005).
4. J. Zhang, K. Fai Mak, N. Nagl, M. Seidel, D. Bauer, D. Sutter, V. Pervak, F. Krausz, and O. Pronin, Light Sci. Appl. **7**, 17180 (2018).
5. G. Vampa, H. Liu, T. F. Heinz, and D. A. Reis, Optica **6**, 553 (2019).
6. J. McNeur, M. Kozák, N. Schönenberger, K. J. Leedle, H. Deng, A. Ceballos, H. Hoogland, A. Ruehl, I. Hartl, R. Holzwarth, O. Solgaard, J. S. Harris, R. L. Byer, and P. Hommelhoff, Optica **5**, 687 (2018).
7. M. Kozak, J. McNeur, K. J. Leedle, H. Deng, N. Schonenberger, A. Ruehl, I. Hartl, J. S. Harris, R. L. Byer, and P. Hommelhoff, Nat. Commun. **8**, 14342 (2017).
8. M. Kozak, J. McNeur, K. J. Leedle, H. Deng, N. Schonenberger, A. Ruehl, I. Hartl, H. Hoogland, R. Holzwarth, J. S. Harris, R. L. Byer, and P. Hommelhoff, Opt. Lett. **41**, 3435 (2016).
9. S. Ghimire, A. D. DiChiara, E. Sistrunk, P. Agostini, L. F. DiMauro, and D. A. Reis, Nat. Phys. **7**, 138 (2010).
10. S. Chaitanya Kumar, A. Esteban-Martin, T. Ideguchi, M. Yan, S. Holzner, T. W. Hänsch, N. Picqué, and M. Ebrahim-Zadeh, Laser Photon. Rev. **8**, L86 (2014).
11. K. Zhao, H. Zhong, P. Yuan, G. Xie, J. Wang, J. Ma, and L. Qian, Opt. Lett. **38**, 2159 (2013).
12. U. Elu, M. Baudisch, H. Pires, F. Tani, M. H. Frosz, F. Köttig, A. Ermolov, P. St. J. Russell, and J. Biegert, Optica **4**, 1024 (2017).
13. S. Antipov, D. D. Hudson, A. Fuerbach, and S. D. Jackson, Optica **3**, 1373 (2016).
14. Z. Qin, G. Xie, J. Ma, P. Yuan, and L. Qian, Photon. Res. **6**, 1074 (2018).
15. Y. Wang, F. Jobin, S. Duval, V. Fortin, P. Laporta, M. Bernier, G. Galzerano, and R. Vallée, Opt. Lett. **44**, 395 (2019).
16. X. Zhu, G. Zhu, C. Wei, L. V. Kotov, J. Wang, M. Tong, R. A. Norwood, and N. Peyghambarian, J. Opt. Soc. Am. B **34**, A15 (2017).
17. Z. Qin, T. Hai, G. Xie, J. Ma, P. Yuan, L. Qian, L. Li, L. Zhao, and D. Shen, Opt. Express **26**, 8224 (2018).
18. Y. Shen, Y. Wang, H. Chen, K Luan, M. Tao, and J. Si, Sci. Rep. **7**, 14913 (2017).
19. M. R. Majewski, R. I. Woodward, and S. D. Jackson, Opt. Lett. **44**, 1698 (2019).

20. O. Henderson-Sapir, S. D. Jackson, and D. J. Ottaway, Opt. Lett. **41**, 1676 (2016).
21. Y. O. Aydın, V. Fortin, F. Maes, F. Jobin, S. D. Jackson, R. Vallée, and M. Bernier, Optica **4**, 235 (2017).
22. J. Li, D. D. Hudson, Y. Liu, and S. D. Jackson, Opt. Lett. **37**, 3747 (2012).
23. P. Tang, Z. Qin, J. Liu, C. Zhao, G. Xie, S. Wen, and L. Qian, Opt. Lett. **40**, 4855 (2015).
24. C. Zhu, F. Wang, Y. Meng, X. Yuan, F. Xiu, H. Luo, Y. Wang, J. Li, X. Lv, L. He, Y. Xu, J. Liu, C. Zhang, Y. Shi, R. Zhang, and S. Zhu, Nat. Commun. **8**, 14111 (2017).
25. Z. Qin, G. Xie, C. Zhao, S. Wen, P. Yuan, and L. Qian, Opt. Lett. **41**, 56 (2016).
26. G. Zhu, X. Zhu, F. Wang, S. Xu, Y. Li, X. Guo, K. Balakrishnan, R. A. Norwood, and N. Peyghambarian, IEEE Photon. Technol. Lett. **28**, 7 (2016).
27. L. Zhao, J. Wang, and S.-W. Huang, in *Advanced Solid-State Photonics* (Optical Society of America, 2018), paper ATu2A.27.
28. S. Duval, M. Bernier, V. Fortin, J. Genest, M. Piché, and R. Vallée, Optica **2**, 623 (2015).
29. T. Hu, S. D. Jackson, and D. D. Hudson, Opt. Lett. **40**, 4226 (2015).
30. R. I. Woodward, D. D. Hudson, A. Fuerbach, and S. D. Jackson, Opt. Lett. **42**, 4893 (2017).
31. S. Duval, M. Olivier, V. Fortin, M. Bernier, M. Piché, and R. Vallée, Proc. SPIE **9728**, 972802 (2016).
32. N. Nagl, K. F. Mak, Q. Wang, V. Pervak, F. Krausz, and O. Pronin, Opt. Lett. **44**, 2390 (2019).
33. P. Wan, L.-M. Yang, S. Bai, and J. Liu, Opt. Express **23**, 9527 (2015).
34. Y. Tang, L. G. Wright, K. Charan, T. Wang, C. Xu, and F. W. Wise, Optica **3**, 948 (2016).
35. S. Vasilyev, I. S. Moskalev, V. O. Smolski, J. M. Peppers, M. Mirov, A. V. Muraviev, K. Zawilski, P. G. Schunemann, S. B. Mirov, K. L. Vodopyanov, and V. P. Gapontsev, Optica **6**, 111 (2019).
36. M. Kozák, M. Förster, J. McNeur, N. Schönenberger, K. Leedle, H. Deng, J. S. Harris, R. L. Byer, and P. Hommelhoff, Nucl. Instrum. Meth. A. **865**, 84 (2017).
37. S. M. J. Kelly, Electron. Lett. **28**, 806 (1992).
38. Y. Cui, F. Lu, and X. Liu, Sci. Rep. **7**, 40080 (2017).
39. X. Liu, D. Popa, and N. Akhmediev, Phy. Rev. Lett. **123**, 093901 (2019).
40. Z. Qin, G. Xie, J. Ma, W. Ge, P. Yuan, L. Qian, L. Su, D. Jiang, F. Ma, Q. Zhang, Y. Cao, and J. Xu, Opt. Lett. **39**, 1737 (2014).
41. Y. Wang, F. Jobin, S. Duval, V. Fortin, P. Laporta, M. Bernier, G. Galzerano, and R. Vallée, Opt. Lett. **44**, 395 (2019).
42. B. Oktem, C. Ülgüdür, and F. Ilday, Nat. Photon. **4**, 307 (2010).
43. X. Liu and Y. Cui, Adv. Photon. **1**, 016003 (2019).
44. F. Gan, J. Non-Cryst. Solids **184**, 9 (1995).
45. C. Agger, C. Petersen, S. Dupont, H. Steffensen, J. K. Lyngsø, C. L. Thomsen, J. Thøgersen, S. R. Keiding, and O. Bang, J. Opt. Soc. Am. B **29**, 635 (2012).
46. D. Tang and L. Zhao, Opt. Lett. **32**, 41 (2007).
47. Y. Zhao, P. Guo, X. Li, and Z. Jin, Carbon **149**, 336 (2019).
48. Z. Hui, W. Xu, X. Li, P. Guo, Y. Zhang, and J. Liu, Nanoscale **11**, 6045 (2019).
49. T. Chai, X. Li, T. Feng, P. Guo, Y. Song, Y. Chen, and H. Zhang, Nanoscale **10**, 17617 (2018).
50. J. Liu, X. Li, Y. Guo, A. Qyyum, Z. Shi, T. Feng, Y. Zhang, C. Jiang, and X. Liu, Small **15**, 1902811 (2019).
51. X. Liu, X. Yao, and Y. Cui, Phys. Rev. Lett. **121**, 023905 (2018).